Reaction of *tert*-butylbenzene (2 equiv) with pyridine-2-aldehyde in concentrated H_2SO_4 gave, after neutralization with NaOH, bis(*p-tert*-butylphenyl)-2-pyridylmethane (85%).[12] Treatment of this compound with equimolar *n*-butyllithium and sulfur in THF at −65 °C followed by warming to room temperature afforded after standard workup Li(*t*-BuL-NS) (59%; **1**, Figure 1). Reaction of **1** (2 equiv) with $MoO_2(acac)_2$[13] gave yellow $MoO_2(t\text{-BuL-NS})_2$ (98%, **2**, Figure 1; ν_{MoO} 901 cm^{-1}, λ_{max} (ϵ_M) 371 (6220) nm). Reaction of **2** with Et_3P (1.5 equiv) in refluxing THF for 5 h yielded brown $MoO(t\text{-BuL-NS})_2$ (69%; **3**, Figure 1; ν_{MoO} 940 cm^{-1}, λ_{max} (ϵ_M) 328 (5210), 430 (3840), 518 (780), 700 (460) nm). Compound **2** has a distorted octahedral structure with cis oxo and trans thiolate ligands, Mo–O = 1.696 (4) Å, O–Mo–O = 107.7 (3)°, and S(1)–Mo–S(1′) = 159.8 (1)°. Compound **3** possesses a distorted trigonal bipyramidal structure with an $MoOS_2$ equatorial plane, axial nitrogen ligands, Mo–O = 1.681 (5) Å, and N(1)–Mo–N(2) = 160.5 (3)°. It is an uncommon example of a five-coordinate $Mo^{IV}O$ complex with physiological-type ligation. Structures and metric parameters[14] are given in Figure 1 from which it is found that the $Mo^{VI}O_2 \rightarrow Mo^{IV}O$ conversion primarily involves large deformations of two bond angles (S–Mo–S by −36°, N–Mo–N by +84°) and significant compression of one bond length (Mo–N by −0.24 Å). It is further evident that the frontside steric hindrance of two *p-tert*-butylphenyl groups in the **2**, and to a lesser extent in **3**, obviates the undesirable formation of a stable, abiological Mo^V–O–Mo^V bridge.[15]

In reaction system II (Figure 1), complex **3** in DMF solution (0.4–1.6 mM) cleanly reduces a variety of substrates. Reactions were monitored spectrophotometrically by the diminution of intensity at 328 and 430 nm and the increase in the 371-nm band of **2**; tight isosbestic points were observed at 341 and 404 nm. Some reactions were also examined by ^1H NMR utilizing the chemical shift differences between the 6-H resonances of **3** (δ 9.52) and **2** (δ 9.37). *Stoichiometric* quantities of the biologically relevant substrates nicotinamide *N*-oxide, adenine *N*-oxide, Me_3NO, and Me_2SO, and also the abiological substrates 3-fluoropyridine *N*-oxide, $(PhCH_2)_3NO$, Ph_2SO, Ph_2SeO, Ph_3AsO, and $NaIO_4$ were reduced. Yields determined in situ from the formation of **2** were in the 81–95% range and can be increased with excess substrate. As already noted, in the reverse reaction **2** is reduced to **3** by Et_3P in good yield.

The intermetal atom transfer reaction **3** + $MoO_2(Et_2dtc)_2 \rightleftarrows$ **2** + $MoO(Et_2dtc)_2$ lies essentially completely to the right, establishing that **3** is a stronger oxo acceptor than $MoO(Et_2dtc)_2$. Given that to date Ph_3AsO is the weakest oxo donor to oxidize **3** and Ph_3P is the weakest oxo acceptor to reduce **2**, the reaction couple **3** + $^1/_2O_2$ = **2** occurs between the couples $Ph_3As + {}^1/_2O_2 = Ph_3AsO$ (ΔH = −43 kcal/mol[16]) and $Ph_3P + {}^1/_2O_2 = Ph_3PO$ (ΔH = −70 kcal/mol[4]) in the thermodynamic scale of oxo transfer reactivity.[4] Thus reaction system II is thermodynamically competent to oxidize or reduce all enzymatic substrates (except those requiring the enzymatic state $Mo^{VI}OS$ as the oxidant). Its stability to the strong oxo donors Me_3NO and IO_4^- is notable.

The kinetics of substrate oxidation in system II have been examined under pseudo-first-order conditions in DMF solutions. Linear plots of rate constants k_1 vs [XO] indicate second-order reactions, and thus a different reaction mechanism from system I,[3,4] and rates sensitive to substrate. For example, at 298 K k_2 = 5.6 (2) × 10^{-2} M^{-1} s^{-1} for XO = Ph_3AsO and k_2 = 1.01 (2) × 10^{-4} M^{-1} s^{-1} for XO = Me_2SO. From the enthalpy[4,16] of the reaction $Ph_3As_{(g)} + Me_2SO_{(g)} \rightarrow Ph_3AsO_{(g)} + Me_2S_{(g)}$, the As–O bond is 16 kcal/mol stronger than the S–O bond, yet the rate of reduction of Ph_3AsO, the more hindered substrate, is 560 times faster.

The synthesis of complexes **2** and **3** facilitates the development of a reaction system whose oxidized and reduced complexes are of known structure, in which the complicating factor of μ-oxo Mo(V) dimer formation is absent in coordinating solvents, and which will transform a broad range of enzymatic and abiological substrates in second-order reactions whose rates are clearly substrate-dependent. System II appears to be the most useful analogue reaction system thus far devised; experiments utilizing it to probe the mechanistic aspects of oxygen atom transfer continue.

Acknowledgment. This research was supported by NSF Grant CHE 89-03283. X-ray diffraction equipment was obtained by NIH Grant 1 S10 RR 02247. We thank M. C. Muetterties for experimental assistance and useful discussions. S.F.G. thanks A. B. Robertson and Co. for financial support.

Supplementary Material Available: Listing of crystal data and atom positional and isotropic thermal parameters and bond angles and distances for compounds **2** and **3** (9 pages). Ordering information is given on any current masthead page.

(12) *Experimental.* Preparations of **2** and **3** were carried out under anaerobic conditions. IR spectra were measured in Nujol or KBr and UV/visible spectra in DMF solutions. All new compounds gave satisfactory elemental analyses and appropriate parent ions in FAB-MS.

(13) Jones, M. M. *J. Am. Chem. Soc.* **1959**, *81*, 3188.

(14) Crystallographic data for compounds **2**·CH_2Cl_2/**3**·3MeCN: a = 23.663 (6)/14.998 (3) Å, b = 17.993 (3)/23.345 (4) Å, c = 13.620 (3)/15.892 (3) Å, β = 118.41 (1)°/93.96 (2)°, T = 173/198 K, space group $C2/c/P2_1/n$, Z = 4 (both), $2\theta_{min/max}$ = 3°–45° (both), unique data ($F_o^2 > 3\sigma F_o^2$) 3652/8078, R, R_w = 5.69, 6.21%/6.38, 6.11%. Data were collected with Mo Kα radiation. Structures were solved by standard procedures; empirical absorption corrections were applied.

(15) Reaction of equimolar **2** and **3** in dichloromethane followed by the addition of ether affords $[Mo(t\text{-Bu-LNS})_2]_2O$ as a dark blue solid, which was identified by the ^1H NMR criterion for a μ-oxo bridged species: Craig, J. A.; Harlan, E. W.; Snyder, B. S.; Whitener, M. A.; Holm, R. H. *Inorg. Chem.* **1989**, *28*, 2024. This compound is fully dissociated in polar solvents such acetonitrile and DMF at the concentrations used in this work.

(16) Barnes, D. S.; Burkinshaw, P. M.; Mortimer, C. T. *Thermochim. Acta* **1988**, *131*, 107.

Driving-Force Effects on the Rates of Bimolecular Electron-Transfer Reactions

T. Mark McCleskey, Jay R. Winkler,* and Harry B. Gray*

Contribution No. 8636, Beckman Institute
California Institute of Technology
Pasadena, California 91125

Received May 18, 1992

The prediction that electron-transfer (ET) rates maximize when the reaction driving force ($-\Delta G°$) equals the reorganization energy (λ) is one of the most intriguing features of ET theory.[1] Consequently, observation of the inverted region ($-\Delta G° > \lambda$) in which rates *decrease* with *increasing* driving force has been a major objective in ET research.[2-10] On the basis of estimated reorg-

(1) Marcus, R. A.; Sutin, N. *Biochim. Biophys. Acta* **1985**, *811*, 265–322.

(2) (a) Calcaterra, L. T.; Closs, G. L.; Miller, J. R. *J. Am. Chem. Soc.* **1983**, *105*, 670–671. (b) Miller, J. R.; Beitz, J. V.; Huddleston, R. K. *J. Am. Chem. Soc.* **1984**, *106*, 5057–5068. (c) Closs, G. L.; Miller, J. R. *Science* **1988**, *240*, 440–447.

(3) Wasielewski, M. R.; Niemczyk, M. P.; Svec, W. A.; Pewitt, E. B. *J. Am. Chem. Soc.* **1985**, *107*, 1080–1082.

(4) McLendon, G.; Miller, J. R. *J. Am. Chem. Soc.* **1985**, *107*, 7811–7816.

(5) (a) Gould, I. R.; Ege, D.; Mattes, S. L.; Farid, S. J. *J. Am. Chem. Soc.* **1987**, *109*, 3794–3796. (b) Gould, I. R.; Moody, R.; Farid, S. J. *J. Am. Chem. Soc.* **1988**, *110*, 7242–7244. (c) Gould, I. R.; Moser, J. E.; Armitage, B.; Farid, S. J. *J. Am. Chem. Soc.* **1989**, *111*, 1917–1919.

(6) (a) Ohno, T.; Yoshimura, A.; Shioyama, H.; Mataga, N. *J. Phys. Chem.* **1987**, *91*, 4365–4370. (b) Asahi, T.; Mataga, N. *J. Phys. Chem.* **1989**, *93*, 6578–6581.

(7) (a) Chen, P.; Duesing, R.; Tapolsky, G.; Meyer, T. J. *J. Am. Chem. Soc.* **1989**, *111*, 8305–8306. (b) Chen, P.; Duesing, R.; Graff, D. K.; Meyer, T. J. *J. Phys. Chem.* **1991**, *95*, 5850–5858.

(8) (a) Macqueen, D. B.; Schanze, K. S. *J. Am. Chem. Soc.* **1991**, *113*, 7470–7479. (b) MacQueen, D. B.; Eyler, J. R.; Schanze, K. S. *J. Am. Chem. Soc.* **1992**, *114*, 1897–1898.

0002-7863/92/1514-6935$03.00/0

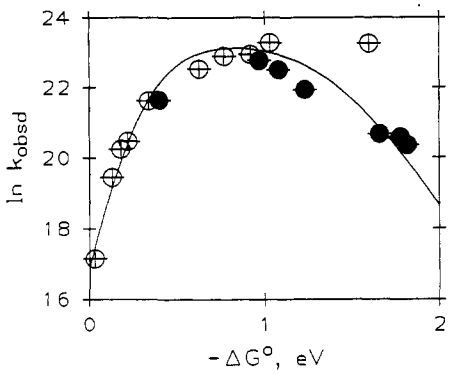

Figure 1. Driving-force dependence of the rates of electron transfer between Ir_2 and various *N*-alkylpyridinium quenchers (py^+) in acetonitrile solution at 25 °C: photoinduced ET reactions (○); thermal recombination reactions (●). Solid curve is a fit of the data to an ET model that includes one quantum-mechanical and one classical reorganization coordinate and corrects for diffusion assuming a limiting rate of 2.5 × 10^{10} M^{-1} s^{-1}. Quenchers used in this work: 2,4,6-trimethyl-*N*-methylpyridinium ($E_{1/2}$ = −1.67 V vs SSCE); 2,3,6-trimethyl-*N*-methylpyridinium (−1.57 V); 2,6-dimethyl-*N*-methylpyridinium (−1.52 V); 2-methoxy-*N*-methylpyridinium (−1.48 V); *N*-ethylpyridinium (−1.36 V); *N*-benzylnicotinamide (−1.07 V); *N*-ethylisonicotinamide (−0.93 V); methyl *N*-methylisonicotinate (−0.78 V); 4-cyano-*N*-methylpyridinium (−0.67 V); 3,4-dicyano-*N*-methylpyridinium (−0.10 V). Preparation of quenchers and electrochemical measurements followed procedures given previously.[12]

anization energies for reactions in solution, it is clear that highly energetic species are necessary to produce ET reactions in the inverted region. The two most common types of energetic reagents used in these studies have been electronically excited molecules and radiolytically generated radicals. Rehm and Weller first examined the driving-force dependence of photoinduced ET reactions (*ET) and found the expected increase in rates at lower driving forces, but instead of decreasing, *ET rates at high driving forces remained pegged at the diffusion limit.[11] Analogous behavior has been observed in many different systems,[12] and only rarely have the "vestiges" of the inverted region been observed in bimolecular *ET reactions.[13-15]

We have extended our work on the *ET reactions between triplet-excited [Ir(1,5-cyclooctadiene)(μ-pyrazolyl)]$_2$ (Ir_2: $Ir_2^{+/*}$ $E_{1/2}$ = −1.7 V vs SSCE; $Ir_2^{+/0}$ $E_{1/2}$ = 0.3 V) and substituted alkylpyridinium acceptors (py^+) to include driving forces as high as 1.6 eV (eq 1; Figure 1, open circles).[12,16] The rates of the

$$*Ir_2 + py^+ \rightarrow Ir^{\bullet+} + py^\bullet \quad (1)$$

$$Ir_2^{\bullet+} + py^\bullet \rightarrow Ir_2 + py^+ \quad (2)$$

recombination (^{b}ET) reactions between $Ir_2^{\bullet+}$ and $py^\bullet$ (eq 2) were also measured using transient absorption spectroscopy.[17] For a simple second-order recombination reaction, $([Ir_2]_0 - [Ir_2])^{-1}$ should vary linearly with reaction time with a slope equal to the second-order rate constant. Plots of $(\Delta Abs)^{-1}$ vs time for four

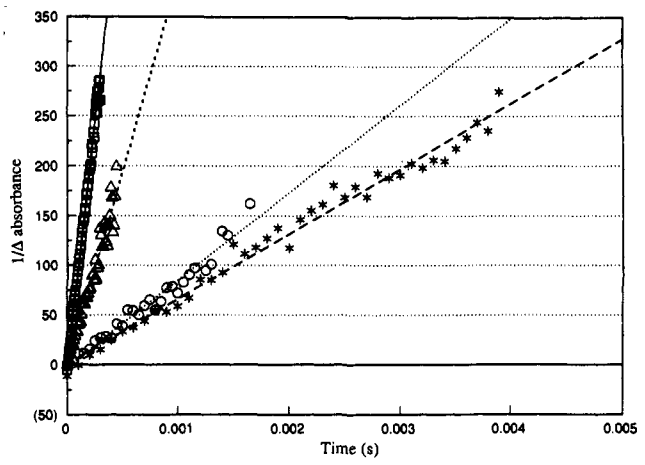

Figure 2. Plots of $[\Delta Abs(500\ nm)]^{-1}$ vs time for recombination reactions of four different quenchers: 4-cyano-*N*-methylpyridinium (□); *N*-ethylisonicotinamide (△); *N*-ethylpyridinium (○); 2,6-dimethyl-*N*-methylpyridinium (*).

different pyridinium quenchers appear in Figure 2. Except at early times (where bandwidth limitations and the first-order generation of $Ir_2^{\bullet+}$ interfere), the plots are very nearly linear. The values of the ^{b}ET rate constants for various pyridinium quenchers are plotted as a function of driving force in Figure 1.[18] These data clearly exhibit an inverted driving-force dependence for $-\Delta G^\circ$ > 1.0 eV. *Even more striking, however, is the observation that at driving forces where ^{b}ET rates are highly inverted, the *ET rates remain diffusion-limited.* The solid curve in Figure 1 is a fit of the *ET and ^{b}ET data (excluding the two highest-driving-force *ET reactions) to an ET model that treats solvent reorganization classically and includes one quantum-mechanical coordinate for inner-sphere reorganization.[19,20] The fit accounts for diffusion effects by assuming a limiting rate constant of 2.5 × 10^{10} M^{-1} s^{-1}. The total reorganization energy estimated for these ET reactions is 0.85 eV.[21]

The solid curve in Figure 1 not only describes the ^{b}ET data but also provides an adequate representation of the *ET data at lower driving forces. Only the diffusion-limited *ET rates appear to deviate from the fit. A possible explanation for this behavior can be found in the electronic structures of pyridinyl radicals. Aromatic π-systems tend to have a closely spaced set of π-bonding orbitals separated by a large energy gap from a closely spaced set of π-antibonding levels. One-electron reduction of such a π-system can lead to radicals with several low-lying states. A calculation of the pyridinyl radical anion electronic structure, for example, places the lowest energy excited state just 0.4 eV above the ground state.[22] It is possible that formation of $*py^\bullet$ radicals preempts inverted behavior in the *ET reactions between $*Ir_2$ and py^+. The formation of electronically excited products is simply another manifestation of inverted driving-force behavior;[23,24]

(9) Zou, C.; Miers, J. B.; Ballew, R. M.; Dlott, D. D.; Schuster, G. B. *J. Am. Chem. Soc.* **1991**, *113*, 7823-7825.
(10) (a) Fox, L. S.; Marshall, J. L.; Gray, H. B.; Winkler, J. R. *J. Am. Chem. Soc.* **1987**, *109*, 6901-6902. (b) Fox, L. S.; Kozik, M.; Winkler, J. R.; Gray, H. B. *Science* **1990**, *247*, 1069-1071.
(11) Rehm, D.; Weller, A. *Isr. J. Chem.* **1970**, *8*, 259-271.
(12) Marshall, J. L.; Stobart, S. R.; Gray, H. B. *J. Am. Chem. Soc.* **1984**, *106*, 3027-3029.
(13) Creutz, C.; Sutin, N. *J. Am. Chem. Soc.* **1977**, *99*, 241-243.
(14) (a) Cho, K. C.; Ng, K. M.; Choy, C. L.; Che, C. M. *Chem. Phys. Lett.* **1986**, *129*, 521-525. (b) Cho, K. C.; Che, C. M.; Ng, K. M.; Choy, C. L. *J. Phys. Chem.* **1987**, *91*, 3690-3693.
(15) Studies of *intramolecular* ET in covalently coupled DA complexes[2-10] have provided compelling evidence for inverted driving-force effects. A curious feature of photoinduced ET in DA complexes, however, is that the inverted effect is observed only for charge-recombination (back) reactions.[3,5,7,10]
(16) The measured yields of cage-separated ET products demonstrate that *ET is the dominant excited-state quenching reaction.
(17) Samples were held in deoxygenated sealed cuvettes and excited with 532-nm, 10-ns, 2-mJ pulses from a Q-switched Nd-YAG laser. Transient absorbance was probed at 500 nm, the absorption maximum of the Ir_2 ground state.[12]
(18) Absolute ^{b}ET rates (k) were extracted from the slopes (m) of the $(\Delta A)^{-1}$ vs time plots according to $k = lm\Delta\epsilon$, where l is the observation pathlength and $\Delta\epsilon$ is the change in molar extinction coefficient at 500 nm. $\Delta\epsilon$(500 nm) was determined by quenching $*Ir_2$ with methyl viologen; the molar absorptivity of the methyl viologen radical cation (ϵ(605 nm) = 12400 M^{-1} cm^{-1}; ϵ(500 nm) = 2820 M^{-1} cm^{-1}) was determined by thin-layer spectroelectrochemistry (for a description of the equipment and procedures see: St. Clair, C. S.; Ellis, W. R.; Gray, H. B. *Inorg. Chim. Acta* **1992**, *191*, 149-155).
(19) The following fitting parameters were used: quantum-mechanical vibrational frequency and reorganization energy, 1600 cm^{-1} and 0.3 eV; classical-coordinate reorganization energy, 0.55 eV.
(20) Brunschwig, B. S.; Sutin, N. *Comments Inorg. Chem.* **1987**, *6*, 209-235.
(21) This reorganization energy agrees well with that extracted from a driving-force study of intramolecular ET in Ir(I) dimers with covalently attached pyridinium acceptors.[10]
(22) Itoh, M.; Okamoto, T.; Nagakura, S. *Bull. Chem. Soc. Jpn.* **1963**, *36*, 1665-1672.
(23) Siders, P.; Marcus, R. A. *J. Am. Chem. Soc.* **1981**, *103*, 748-752.
(24) Kikuchi, K.; Katagiri, T.; Niwa, T.; Takahashi, Y.; Suzuki, T.; Ikeda, H.; Miyashi, T. *Chem. Phys. Lett.* **1992**, *193*, 155-160.

formation of *py•, though energetically less favorable, is faster than formation of py•. In the case of back reactions, the lowest electronic excited states of Ir_2 and py^+ are too energetic to be formed in recombination reactions, and inverted behavior is observed.

Regardless of the disparity between the *ET and bET reactions, our data demonstrate that inverted driving-force effects can be observed in *bimolecular* ET reactions. The appearance of inverted effects only for bET reactions may be a feature common to many of the other bimolecular ET systems that have been studied. If formation of electronically excited products is indeed the reason for this disparity, then it should be possible to select donors and acceptors that exhibit inverted driving-force effects in bimolecular photoinduced ET reactions as well.

Acknowledgment. T.M.M. acknowledges a National Science Foundation graduate fellowship and a fellowship from the Department of Education (Graduate Assistance in Areas of National Need). This research was supported by National Science Foundation Grant CHE-8922067.

Supplementary Material Available: Table of rates and driving forces for photoinduced ET and thermal recombinations (1 page). Ordering information is given on any current masthead page.

Haloalkanes as Ligands. Spectroscopic and Energetic Studies of $CpMn(CO)_2XR$

Ping-Fan Yang and Gilbert K. Yang*

Department of Chemistry
University of Southern California
Los Angeles, California 90089-0744

Received June 1, 1992

A number of metal complexes containing chloro-, bromo- or iodocarbons ligated through the halide atom have been prepared and, in several instances, characterized by X-ray diffraction.[1,2] While many of these complexes involve chelation of a bound ligand, it is evident that coordination of a haloalkane in an intermolecular fashion is possible. O'Driscoll and Simon have shown that coordination of an alkyl halide to a transition metal complex is a rapid process, complete within 5 ns of light absorption.[3] Recent gas-phase studies by Bogdan, Wells, and Weitz have found that the Cl-W bond strength in $ClF_2CCl-W(CO)_5$ is 19.7 ± 0.6 kcal/mol.[4]

We have found that coordination of a number of haloalkanes (RX) to the formally 16e⁻ $CpMn(CO)_2$ moiety occurs readily.[5] These complexes have been characterized at low temperature by FTIR and UV/visible spectroscopies, and the Mn-XR bond strengths have been probed by time-resolved photoacoustic calorimetry.

Photolysis ($\lambda < 400$ nm) of $CpMn(CO)_3$ (**1**) in donor solvents such as THF leads to formation of the solvate $CpMn(CO)_2(THF)$ (**3**-THF).[6] The coordinatively unsaturated intermediate **2** is presumably involved. Donor molecules present in solution rapidly displace THF from **3**-THF to yield **4** (Scheme I).[6] At low temperature in the absence of L, the solvated species **3** have sufficient lifetimes to be characterized spectroscopically. Thus, photolysis of $CpMn(CO)_3$ in the presence of a wide variety of haloalkanes at 195 K allows spectroscopic characterization of $CpMn(CO)_2S$ (**3**-XR). These results are summarized in Table I.

Scheme I

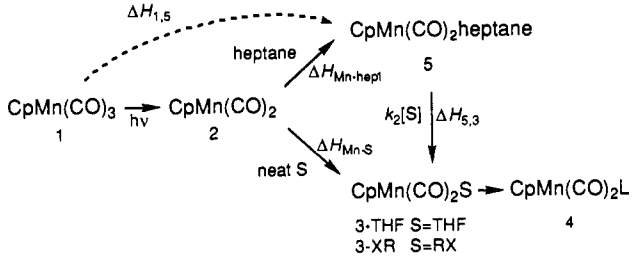

The difference FTIR and UV/visible spectra are very similar for photolyses of $CpMn(CO)_3$ in different neat haloalkane solutions. In the infrared spectrum at 195 K, bleaching of the starting material absorbances at 1932 and 2021 cm^{-1} is observed together with the appearance of a single new absorption at ~1870 cm^{-1}. Except for the photolyses in CH_2Cl_2, a second band is obscured by the intense starting material band at 1932 cm^{-1}. In neat CH_2Cl_2 solution the higher energy band is shifted away from the starting material absorption and appears at 1946 cm^{-1}. The difference UV/visible spectra display new absorptions with λ_{max} = ~395 and ~500 nm. These absorption maxima are consistent with the appearance of a bright red color during preparative scale photolyses. Complex **3**-THF shows a new CO absorption at 1845 cm^{-1}, with a second band at ~1932 cm^{-1} hidden by the starting material absorption. Two new intense visible absorptions appear at $\lambda_{max}(\epsilon_{rel})$ = 390(1.1) and 507(1.0) nm. These spectral data agree well with those reported in the literature.[7,8] Photolyses of $CpMn(CO)_3$ in hexane solutions of the haloalkanes (1.0-2.5 M) at 195 K led to results similar to those obtained in neat haloalkane solutions with only slight shifts of the ν_{CO} bands to higher frequency. These bands are significantly different from ν_{CO} observed in neat hydrocarbon matrix at 12 K,[9] in hydrocarbon glass at 77 K,[8,10,11] and in heptane solution at 293 K.[12] The ν_{CO} and λ_{max} values are also different from those of the absorptions assigned to $Cp_2Mn_2(CO)_5$ resulting from the reaction of **2** with **1**.[13] Low-temperature studies in CH_2Br_2 solution were not possible because of its high freezing point and low solubility in hexanes at 195 K.

While the IR and UV/visible spectra were consistent with assignment of **3**-XR as complexes of the type $CpMn(CO)_2XR$, chemical confirmation was needed to support this spectroscopic result. To justify the formulation of **3**-XR as $CpMn(CO)_2XR$ and to demonstrate the weak nature of the M-XR interaction, PMe_3 was added to neat haloalkane solutions of **3**-XR at 195 K. Over several hours the bright red color of the haloalkane complexes was replaced by a bright yellow color, and $CpMn(CO)_2PMe_3$ was isolated as the unique product in high yield.[14] This reaction

(1) For an excellent recent review, see: Kulawiec, R. J.; Crabtree, R. H. *Coord. Chem. Rev.* **1990**, *99*, 89-115.
(2) See also: (a) Fernández, J. M.; Gladysz, J. A. *Inorg. Chem.* **1986**, *25*, 2672-2674. (b) Fernández, J. M.; Gladysz, J. A. *Organometallics* **1989**, *8*, 207-219 and references cited therein. (c) Winter, C. H.; Veal, W. R.; Garner, C. M.; Arif, A. M.; Gladysz, J. A. *J. Am. Chem. Soc.* **1989**, *111*, 4766-4776. (d) Kulawiec, R. J.; Faller, J. W.; Crabtree, R. H. *Organometallics* **1990**, *9*, 745-755. (e) Colsman, M. R.; Newbound, T. D.; Marshall, L. J.; Noirot, M. D.; Miller, M. M.; Wulfsberg, G. P.; Frye, J. S.; Anderson, O. P.; Strauss, S. H. *J. Am. Chem. Soc.* **1990**, *112*, 2349-2362. (f) Bown, M.; Waters, J. M. *J. Am. Chem. Soc.* **1990**, *112*, 2442-2443. (g) Gomes-Carneiro, T. M.; Jackson, R. D.; Downing, J. H.; Orpen, A. G.; Pringle, P. G. *J. Chem. Soc., Chem. Commun.* **1991**, 317-319.
(3) O'Driscoll, E.; Simon, J. D. *J. Am. Chem. Soc.* **1990**, *112*, 6580-6584.
(4) Bogdan, P. L.; Wells, J. R.; Weitz, E. *J. Am. Chem. Soc.* **1991**, *113*, 1294-1299.
(5) Casey and Fraley have prepared $(\overline{BrCH_2CH_2Cp})Mn(CO)_2$, which contains an intramolecularly bound bromine atom. Fraley, M. E.; Casey, C. P. Personal communication of unpublished results.
(6) (a) Strohmeier, W. *Angew. Chem., Int. Ed. Engl.* **1964**, *3*, 730-737. (b) Caulton, K. G. *Coord. Chem. Rev.* **1981**, *38*, 1-43.
(7) Giordano, P. J.; Wrighton, M. S. *Inorg. Chem.* **1977**, *16*, 160-166.
(8) Black, J. D.; Boylan, M. J.; Braterman, P. S. *J. Chem. Soc., Dalton Trans.* **1981**, 673-677.
(9) Rest, A. J.; Sodeau, J. R.; Taylor, D. J. *J. Chem. Soc., Dalton Trans.* **1978**, 651-656.
(10) Hill, R. H.; Wrighton, M. S. *Organometallics* **1987**, *6*, 632-638.
(11) Bitterwolf, T. E.; Lott, K. A.; Rest, A. J.; Mascetti, J. *J. Organomet. Chem.* **1991**, *419*, 113-126.
(12) Creaven, B. S.; Dixon, A. J.; Kelly, J. M.; Long, C.; Poliakoff, M. *Organometallics* **1987**, *6*, 2600-2605.
(13) Data for $Cp_2Mn_2(CO)_5$: $\lambda_{max}(\epsilon_{rel})$ = 360(1.7), 530(1.0) nm; ν_{CO} (heptane, 293 K), terminal CO, 1993, 1955, 1934, 1907 cm^{-1}; bridging CO, 1777 cm^{-1}; ^{13}CO satellite, 1740 cm^{-1}. Data from ref 12.

0002-7863/92/1514-6937$03.00/0